Measurement of the Structure Function F_L by the H1 collaboration

Sasha Glazov

DESY
Notkestrasse 85,
22607 Hamburg, Germany

New measurement of the structure function F_L performed at the HERA collider by the H1 collaboration is reported. The result is based on the neutral current inclusive e^+p scattering cross section collected at a positron beam energy of 27.6 GeV and proton beam energies at 460, 575 and 920 GeV. Using the H1 backward silicon tracker, the measurement extends towards a low value of the absolute four momentum transfer squared $Q^2 = 2.5$ GeV^2.

At low absolute four momentum transfer squared Q^2, the inclusive double differential ep scattering cross section in a reduced form can be represented by two structure functions:

$$\sigma_r(x,Q^2) = F_2(x,Q^2) - f(y)F_L(x,Q^2), \qquad f(y) = \frac{y^2}{Y_+}, \quad Y_+ = 1 + (1-y)^2. \tag{1}$$

Here x is the Bjorken scaling variable, and the inelasticity y is related with x, Q^2 and the centre-of-mass energy squared S as $y = Q^2/(Sx)$. The structure functions F_2 and F_L correspond to the scattering cross sections for transversely and longitudinally polarised photons: $F_2 \sim \sigma_T + \sigma_L$ and $F_L \sim \sigma_L$. The ratio of σ_L and σ_T defines a function R which can be used instead of F_L. Due to the kinematic factor $f(y)$ and the relation $0 \leq F_L \leq F_2$, the F_L term has a numerically significant influence on the cross section only for $y > 0.5$. An event at high inelasticity, reconstructed in the H1 detector, is shown in figure 1.

In the quark parton model for massless spin 1/2 quarks $\sigma_L = 0$ is predicted from angular momentum conservation. In NLO DGLAP [2], gluon emission weakens the angular momentum restriction and F_L acquires a non-zero value. Measuring F_L thus allows for the determination of the gluon density using the cross section helicity decomposition.

At low Q^2 and low x the gluon density shows rapid evolution. It has been estimated that higher order corrections become significant for F_L[3]. In addition, large $\ln 1/x$ terms may have important contributions[4]. This leads to a considerable spread of theoretical predictions for F_L, increasing interest in making measurements in this kinematic domain.

To determine the two structure functions $F_2(x,Q^2)$ and $F_L(x,Q^2)$ from the reduced cross section, equation 1, it is necessary to perform measurements at the same values of x and Q^2 but different y. This is achieved at HERA by reducing the proton beam energy. Two runs at reduced proton beam energy $E_p = 460$ GeV and $E_p = 575$ GeV were performed with an integrated luminosity of about 13 and 6 pb^{-1}, respectively. The run at $E_p = 460$ GeV gives highest sensitivity to F_L while the run at $E_p = 575$ GeV extends the kinematic range of the measurement and provides an important cross check.

The measurement must extend to as high y as possible to increase sensitivity to F_L. A high y kinematic domain at low Q^2 corresponds to low energies of the scattered positron E'_e. Measurement at low E'_e is challenging primarily because of high hadronic background. To reduce and estimate this background the positron candidate must have a reconstructed track

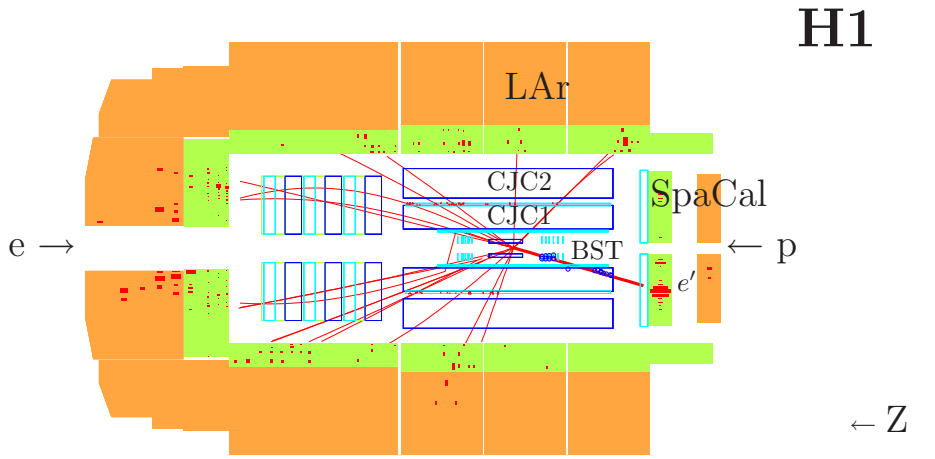

Figure 1: A view of a high y event reconstructed in the H1 detector. The positron and proton beam directions are indicated by the arrows. For the coordinate system used at HERA the z axis points in the direction of the proton beam. The interaction vertex is reconstructed using the hadronic final state (thin lines) and the scattered positron (thick line) tracks in the central tracker. The central tracker consists of (from the beam line outwards) the silicon tracker, the drift chambers CJC1 and CJC2, it is surrounded by the liquid argon (LAr) calorimeter. The detector operates in a solenoidal magnetic field of 1.16 T. The scattered positron trajectory is reconstructed in the backward silicon tracker BST and the CJC1. The charge of the particle is determined using the track curvature. The positron energy is measured in the electromagnetic part of the SpaCal calorimeter.

with well determined curvature. The H1 collaboration published the first measurement of F_L at HERA using drift chambers CJC1 and CJC2 together with the SpaCal calorimeter for $12 \leq Q^2 \leq 90$ GeV^2[5] and also reported a preliminary result at higher Q^2 using the LAr calorimeter[6]. Here the new preliminary result using the silicon tracker BST is reported.

In order to validate the scattered positron at low Q^2 a dedicated tracking algorithm is developed which combines hit information from the BST and CJC trackers. This algorithm ensures high and uniform reconstruction efficiency of the particle charge for $Q^2 \geq 2.5$ GeV^2. For the scattered lepton the reconstructed charge is expected to coincide with the lepton beam charge (positive for the runs with reduced E_p). The sample with the charge opposite to the beam provides the background sample. Assuming charge symmetry of the background, this opposite charge sample may be subtracted from the correct charge sample to obtain the DIS signal. There is, however, a small charge asymmetry of the background which arises from a difference in the SpaCal calorimeter response to particles compared to anti-particles. This asymmetry is measured directly from data using runs with different beam charge and also samples of pure background events in which the true scattered positron is detected at low angles in the electron tagger calorimeter. Figure 2 shows comparison of the distributions of the main kinematic variables in data and DIS Monte Carlo simulation (MC). The background increases very rapidly for high y, however, a data driven determination allows to estimate it reliably.

The structure function F_L is measured as a slope of a linear fit of $\sigma_r(x, Q^2, f(y))$ versus $f(y)$. These fits are shown in figure 3 for $Q^2 = 5$ GeV^2. For this Q^2 bin, the uncertainty on F_L is smallest for $x = 0.00012$ and $x = 0.00013$ which correspond to $y = 0.85$ and $y = 0.75$

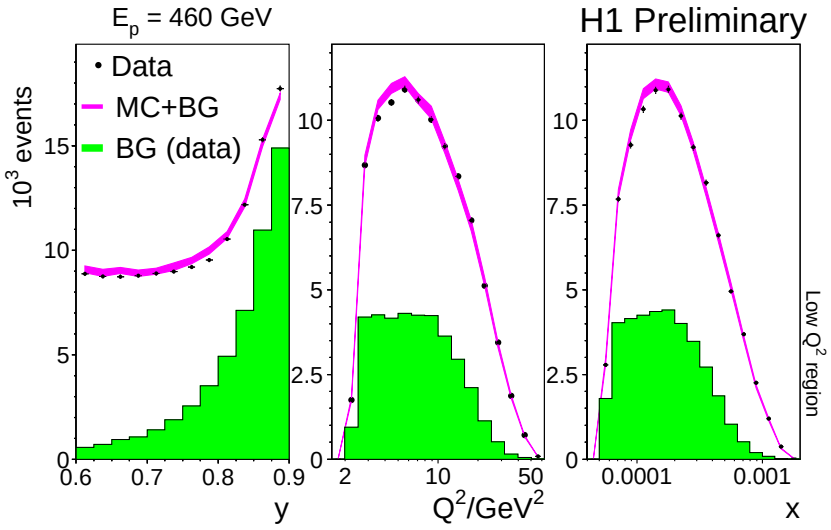

Figure 2: Distribution of the main kinematic variables y (left), Q^2 (centre) and x (right) compared between data (dots with error bars) and sum of DIS MC (error band) and data-driven background estimation (hashed histogram). The error bands include MC and background statistical uncertainties as well as systematic uncertainty.

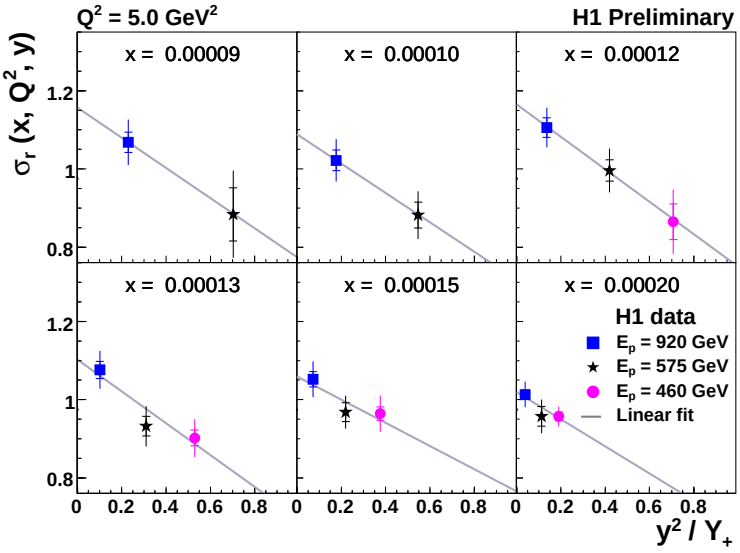

Figure 3: Reduced cross section measured by the H1 collaboration for $Q^2 = 5$ GeV^2 and different x as a function of $f(y)$. The H1 data taken with $E_p = 920$, 575 and 460 GeV are shown as square, star and circle symbols with error bars (inner: statistical, outer: total). The lines show linear fits to the data to determine F_L.

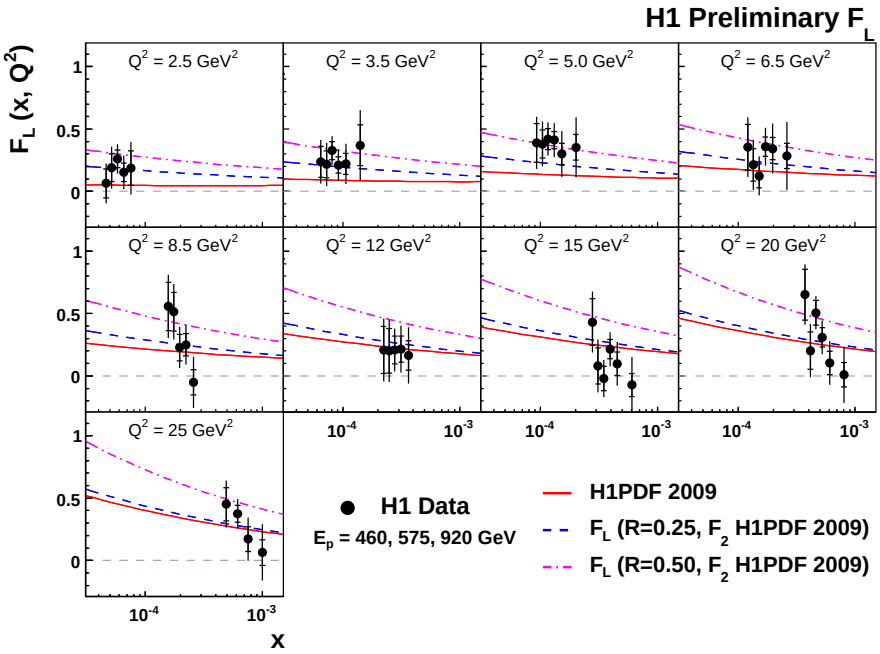

Figure 4: Measurement of the structure function F_L at low Q^2. The H1 data shown as dots with error bars (inner: statistical, outer: total) compared to prediction of the H1PDF2009 fit[7], shown as solid line, and F_L calculated using F_2 from the H1PDF2009 prediction and $R = 0.25$ ($R = 0.50$), shown as dashed (dashed-dotted) line.

for the $E_p = 460$ GeV data. The structure function F_L measured by the H1 collaboration using the BST-CJC and SpaCal is shown in figure 4. For $Q^2 \geq 12$ GeV^2, the data agree well with the published result[5] and improve coverage to higher x for $Q^2 \leq 15$ GeV^2. The measurement covers $2.5 \leq Q^2 \leq 8.5$ GeV^2 kinematic range for the first time at HERA. For low Q^2, the data lie above the prediction derived from the QCD fit to H1 data, H1PDF 2009[7] and agree well with F_L calculated as $F_L = R/(1+R)F_2$ with $R = 0.25$ and F_2 taken from the H1PDF2009 fit.

The range in x covered by the measurements for each Q^2 bin is limited, and for this range the expected variation of F_L is small. Therefore, the measurements are averaged for each Q^2 bin in order to obtain a more compact representation of the data. For $Q^2 \geq 35$ GeV^2 the precision of F_L is improved if the data from the SpaCal and LAr based analyses are combined, therefore the preliminary results from[6] are used here.

The combined averaged data are compared to DGLAP QCD based predictions and various models in figure 5 left and right, respectively. The data agree well with predictions for $Q^2 \geq 10$ GeV^2. For lower Q^2 there is, however, a larger spread between models and the data tend to be higher than several of them. Among DGLAP models, the data agree better with CTEQ[8] and Alekhin[9] compared to MSTW[10] and H1PDF2009. The difference between NLO DGLAP models can be understood as an effect of higher order corrections since the MSTW fit uses terms sub-leading in α_S for calculation of F_L which turn out to be negative at NLO and H1PDF2009 uses the code of MSTW. For phenomenological models, the data

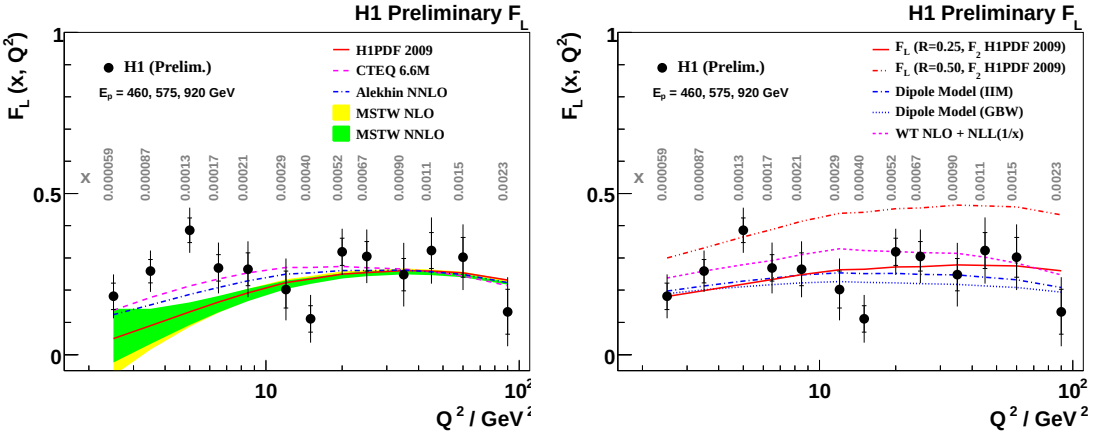

Figure 5: Combined averaged structure function F_L as function of Q^2. The corresponding x values are shown in grey. The H1 data are shown as circles with error bars (inner: statistical, outer: total) compared to predictions of (left figure) the H1PDF2009 fit[7] (solid line), CTEQ[8] (dashed line), Alekhin[9] (dashed-dotted line) MSTW[10] at NLO (lighter error band), MSTW at NNLO (darker error band) as well as (right figure) F_L calculated using fixed $R = 0.25$, 0.5 and F_2 from the H1PDF2009 fit (solid and dashed-double dotted line), Dipole Models[11] (doted and dashed-dotted line) and resummed WT model[4] (dashed line).

agree well with the simple $R = 0.25$ assumption as well as with predictions from two Dipole model fits to the H1 data collected at $E_p = 920$ GeV[11]. For $Q^2 \leq 10$ GeV^2 the data agree the best with White Thorne (WT) prediction which includes $\ln 1/x$ resummation, however for $12 \leq Q^2 \leq 15$ GeV^2 this model overshoots the data.

References

[1] Slides:
`http://indico.cern.ch/materialDisplay.py?contribId=42&sessionId=0&materialId=slides&confId=53294`

[2] V.N. Gribov and L.N. Lipatov, Sov. J. Nucl. Phys. 15 (1972) 438;
V.N. Gribov and L.N. Lipatov, Sov. J. Nucl. Phys. 15 (1972) 675;
L.N. Lipatov, Sov. J. Nucl. Phys. 20 (1975) 94;
Y.L. Dokshitzer, Sov. Phys. JETP 46 (1977) 641;
G. Altarelli and G. Parisi, Nucl. Phys. B 126 (1977) 298.

[3] S.Moch, J.A.M. Vermaseren and A. Vogt, Phys. Lett. B606 (2005) 123.

[4] C.D. White and R.S. Thorne, Phys. Rev. D 75, 034005 (2007).

[5] F. Aaron *et al.* [H1 Collaboration], Phys. Lett. B 665 (2008) 139.

[6] V. Chekelian [for the H1 Collaboration], "Direct F_L Measurement at Hiqh Q^2 at HERA", Proc. of XVI Int. Workshop on Deep-Inelastic Scattering and Related Topics, London, England, April 2008

[7] F. Aaron *et al.* [H1 Collaboration], arXiv:0904.3513, submitted to EPJC.

[8] P.M. Nadolsky *et al.* Phys. Rev. D 78, 013004 (2008).

[9] S. Alekhin. JETP Lett. 82 (2005) 628.

[10] A.D. Martin, W.J. Stirling, R.S. Thorne and H. Watt, Phys. Lett. B652 (2007) 292.

[11] F. Aaron *et al.* [H1 Collaboration], arXiv:0904.0929, submitted to EPJC.